PNAS RESEARCH ARTICLE | MICROBIOLOGY

Soil microbiome bacteria protect plants against filamentous fungal infections via intercellular contacts

Long Lin[a], Danyu Shen[a], Xiaolong Shao[a], Yicheng Yang[a], Li Li[b], Caihong Zhong[b], Jiandong Jiang[c], Mengcen Wang[d,e], and Guoliang Qian[a,1]

Affiliations are included on p. 11.

Edited by Jeffery Dangl, The University of North Carolina at Chapel Hill, Chapel Hill, NC; received September 13, 2024; accepted December 6, 2024

Bacterial–fungal interaction (BFI) has significant implications for the health of host plants. While the diffusible antibiotic metabolite-mediated competition in BFI has been extensively characterized, the impact of intercellular contact remains largely elusive. Here, we demonstrate that the intercellular contact is a prevalent mode of interaction between beneficial soil bacteria and pathogenic filamentous fungi. By generating antibiotics-deficient mutants in two common soil bacteria, *Lysobacter enzymogenes* and *Pseudomonas fluorescens*, we show that antibiotics-independent BFI effectively inhibits pathogenic fungi. Furthermore, transcriptional and genetic evidence revealed that this antibiotics-independent BFI relies on intercellular contact mediated by the type VI secretion system (T6SS), which may facilitate the translocation of bacterial toxic effectors into fungal cells. Finally, by using a "conidia enrichment" platform, we found that T6SS-mediated fungal inhibition resulting from intercellular contact naturally occurs within the soil microbiome, particularly represented by *Pseudomonas fulva*. Overall, these results demonstrate that bacteria from the soil microbiome can protect host plants from fungal infection through antibiotics-independent intercellular contacts, thus revealing a naturally occurring and ecologically important mode of BFI in agricultural contexts.

bacterial–fungal interaction | filamentous fungi | contact-dependent antifungal activity | T6SS

Significance

Soil bacteria are widely recognized for their ability to inhibit fungal pathogens and protect plants through the production of diffusible antibiotic metabolites, a mechanism that does not necessitate direct intercellular contact between bacteria and fungi. Here, we present an antifungal phenomenon in which effective inhibition is contingent upon intercellular contacts between bacterial cells and conidia of filamentous fungi. This contact-dependent antifungal activity functions independently of antibiotics and is mediated by type VI secretion system (T6SS) in bacteria, represented by *Lysobacter* and *Pseudomonas*. These findings expand our understanding of the inhibitory effects of T6SS beyond its previously recognized influence on yeast-like fungi, thus offering strategies for the identification of biocontrol bacteria to safeguard crop health.

Phytopathogenic fungi pose a significant threat to global crop production, accounting for 30% of crop yield losses and contamination issues arising from mycotoxins (1, 2). Bacterial–fungal interactions (BFIs) are crucial factors for ecosystem functioning and health (3). The mechanisms underlying BFIs offer promising solutions for the effective control of fungal diseases in agricultural settings (4). Bacteria residing in bulk soil and the rhizosphere act as formidable competitors against pathogenic fungi, thereby serving as valuable microbial resources for the discovery of antibiotics. BFIs mediated with the naturally transmitted-antibiotics have thus far been regarded as a typical contact-independent interaction model between bacteria and filamentous fungi.

As prevalent members of gram-negative bacteria in the plant's belowground compartments, the genera *Pseudomonas* and *Lysobacter* produce and secrete various antibiotic metabolites that serve as antifungal weapons (5–7). Within *Pseudomonas*, phenazine-1-carboxylate and 2,4-diacetylphloroglucinol (2,4-DAPG) have been identified as effective fungicidal compounds (6, 8). *Lysobacter* bacteria exhibit broad-spectrum inhibitory effects against crop fungal pathogens by generating distinct antimicrobial substances, including the heat-stable antifungal factor (HSAF) (9–11). Notably, recent evidence suggests that contact-dependent antibacterial mechanisms are widespread among the bacterial competitors, with the type VI secretion system (T6SS) and type IV secretion system (T4SS) being the most commonly utilized in gram-negative bacteria (12).

Following cell-to-cell contact within bacterial community, bacteria exhibiting T6SS/T4SS activity can eliminate competitor cells by injecting lethal effector proteins. This interspecies killing behavior relies on direct cell-to-cell contact, rather than the production of antibiotic metabolites (12, 13). Previous studies have demonstrated that *L. enzymogenes* is incapable of producing antibiotic metabolites against gram-negative bacteria. However, it can efficiently eliminate bacterial competitors via a contact-dependent mechanism mediated by the T4SS (14, 15). The coculture of bacterial cells utilized in these case studies has established a standardized approach to simulate the natural cell-to-cell interactions inherent in bacterial interspecies dynamics, which have also been adapted to observe contact-dependent BFIs between bacteria and ecologically related fungi, including both yeast and filamentous-form of yeast-like fungi (16, 17). In contrast, phytopathogenic filamentous fungi exhibit more complex structures than yeast-like fungi, possessing multicellular and intricate hyphae, which complicate the study of intercellular contacts within BFIs (3). Consequently, it remains unclear whether

Author contributions: C.Z., J.J., and G.Q. designed research; L. Lin, X.S., Y.Y., and L. Li performed research; L. Lin and D.S. analyzed data; and L. Lin, X.S., M.W., and G.Q. wrote the paper.

The authors declare no competing interest.

This article is a PNAS Direct Submission.

[1]To whom correspondence may be addressed. Email: glqian@njau.edu.cn.

This article contains supporting information online at https://www.pnas.org/lookup/suppl/doi:10.1073/pnas.2418766122/-/DCSupplemental.

Published January 15, 2025.

and how bacteria utilize intercellular contact-dependent secretion systems to engage with filamentous pathogenic fungi in agricultural contexts.

To establish a laboratory condition that simulates the natural contact-dependent interactions between bacteria and filamentous fungi, we developed a coculture system involving bacterial cells and conidia of filamentous fungi grown on solid media. Utilizing this system, we found that the antibiotics-deficient mutants of *L. enzymogenes* and *P. fluorescens* effectively inhibited the growth of various filamentous fungi. Furthermore, we provided transcriptional, genetic, and biochemical evidence demonstrating that the antibiotic-independent antifungal activity exhibited by *L. enzymogenes* and *P. fluorescens* is dependent on T6SS-mediated intercellular contacts. Finally, we established a "conidia enrichment" platform to demonstrate that T6SS-mediated fungal inhibition, triggered by intercellular contact, occurs naturally within the soil microbiome. This phenomenon appears to represent an interkingdom BFI model in agricultural settings.

Results

***L. enzymogenes* Inhibits Fungal Growth via Antibiotic-Independent Intercellular Contact.** To investigate the potential of soil bacteria in employing contact-dependent killing mechanisms to suppress the growth of filamentous fungi without antibiotic metabolites, we selected *L. enzymogenes* OH11, a biocontrol bacterium recognized for its ability to protect various crops against fungal infections by secreting the well-characterized antifungal antibiotic HSAF (18) (Fig. 1*A*). Using a dual-culture assay (antagonistic assay), we observed that wild-type (WT) OH11 displayed significant antifungal activity against the model phytopathogenic fungus *Fusarium graminearum* PH-1, whereas the HSAF-deficient mutant Δ*lafB* (a mutant of the first gene in the HSAF biosynthetic operon) exhibited a near-complete loss of antifungal activity (Fig. 1*B*). Similarly, the Δ*lafB* mutant did not demonstrate antagonistic activity against three other filamentous fungal pathogens that we tested—*Fusarium oxysporum*, *Alaternaria alternata* and *Colletotrichum gloeosporioides* (*SI Appendix*, Fig. S1), suggesting that HSAF is crucial for contact-independent antifungal effects. However, the Δ*lafB* spots were not entirely covered by fungi (Fig. 1*B* and *SI Appendix*, Fig. S1), indicating that *L. enzymogenes* may inhibit fungal growth in an HSAF-independent mechanism following directly made contact with fungal cells. To explore this further, we used *F. graminearum* PH-1 as our working model. We cocultured cells of WT OH11 or HSAF-deficient mutant (Δ*lafB*), both in 10% TSB (OD_{600} = 1.0), with PH-1 conidia (200 conidia/μL) on 10% TSA agar plates to replicate intercellular contact between bacteria and fungi. We observed complete inhibition of PH-1 growth, from conidial germination to mature hypha formation, in the presence of both OH11 and Δ*lafB*. Notably, the fungal growth inhibition associated with Δ*lafB* was completely abolished when Δ*lafB* cells and PH-1 conidia were separated by a 0.22-μM PVDF filter membrane, which effectively prevented intercellular contact (Fig. 1*C*). In contrast, only the WT OH11 was able to produce HSAF after isolated growth, which allowed it to "penetrate" the membranes and inhibit fungal growth (Fig. 1*C*). Furthermore, we inoculated OH11 or Δ*lafB* cells suspended in water with PH-1 conidia on PDA plates which were positioned at varying distances. The result indicated that WT OH11 could inhibit the mycelial growth of PH-1 even before direct intercellular contact occurred, while Δ*lafB* only exhibited inhibitory effects after direct contact was established (Fig. 1*D*). These findings suggested that *L. enzymogenes* inhibits fungal growth through intercellular contact in an HSAF-independent manner, indicating that this contact-dependent antifungal effect did not necessitate cell-to-cell mixing from the outset.

To substantiate these observations at the molecular level, we conducted RNA-seq assays to identify fungal genes whose transcription was significantly altered upon contact with *L. enzymogenes* cells, independent of HSAF. We prepared a water suspension of Δ*lafB* cells, mixed it with PH-1 conidia, and inoculated the mixture on PDA agar plates 24 h prior to RNA-seq analysis. The results indicated that the coculture of HSAF-deficient mutant cells notably affected fungal gene expression compared to the negative control (H_2O-treated). We identified 981 DEGs that were up-regulated and 684 genes down-regulated (*SI Appendix*, Fig. S2 and Dataset S1). These DEGs were predominantly enriched in categories related to metabolic process, catalytic activity, and membrane Gene Ontology (GO) terms. Additionally, several genes associated with stimulus responses (35 genes), transporter activity (136 genes), antioxidant activity (13 genes), and transcription factors (47 genes) were also differentially expressed (Fig. 1*E*). Specifically, 27 DEGs involved in ubiquinone and other terpenoid-quinone biosynthesis and 57 DEGs related to porphyrin metabolism were identified by KEGG annotation (*SI Appendix*, Fig. S2). Furthermore, we identified 11 DEGs involved in glycerophospholipid metabolism, which have been recognized as essential for fungal cell membrane biogenesis (19) (*SI Appendix*, Fig. S2). These findings demonstrate that the transcription of fungal genes associated with membrane and metabolic processes is broadly influenced by intercellular contact with *L. enzymogenes*. An earlier study indicated that HSAF induced cell wall thickening and plasmolysis, resulting in the abnormal germination of PH-1 conidia (20). BarA, a ceramide synthase involved in sphingolipid signaling, has been identified as a potential target of HSAF (21–23). It has been demonstrated that HSAF treatment alters the expression of multiple genes in *Alternaria alternata*, including those involved in sphingolipid metabolism and signaling pathway, chitin synthase, and the key central protein phosphatase 2A (24). With the exception of two chitin synthase genes, none of aforementioned genes exhibited differential expression in our observations. The DEGs of PH-1 induced by exposure to Δ*lafB* were primarily associated with the biosynthesis of cell membrane and organelle, rather than the cell wall, suggesting that *L. enzymogenes* may target *F. graminearum* through a contact-dependent inhibitory mechanism distinct from those mediated by HSAF. The expression levels of several selected genes involved in PH-1 conidia production and germination regulation were validated by qRT-PCR, including *FGSG_01176* (FgSR, transcription factor), *FGSG_04770* (kinase), *FGSG_08701* (Gin4-like kinase), *FGSG_01641* (kinase), *FGSG_03846* (TAG lipases), and FGSG_*06610* (phosphatases) (25–27) (Fig. 1*F*). We selected fungal mutants of 4 DEGs (*FgSR*, *FGSG_01641*, *FGSG_04770,* and *FGSG_08701*) to genetically correlate the RNA-seq data with contact-dependent antifungal effects. Through coculture experiments, we observed that one of the fungal mutants (Δ*FGSG_08701*) displayed a colony size similar to that of the WT PH-1 when grown in isolation. However, its growth was more susceptible to inhibition by Δ*lafB* (*SI Appendix*, Fig. S3), thereby providing further support for the RNA-seq results.

To determine whether the observed intercellular contact-dependent inhibition of fungal growth by *L. enzymogenes* is a widespread phenomenon or specific to certain fungal species, we further prepared conidia from three additional fungi (*F. oxysporum*, *A. alternata,* and *C. gloeosporioides*) and mixed them with cells of the WT OH11 or HSAF-deficient mutant, respectively. The results demonstrated that fungal growth inhibition occurred when all tested conidia were cocultured with either WT OH11 or Δ*lafB*.

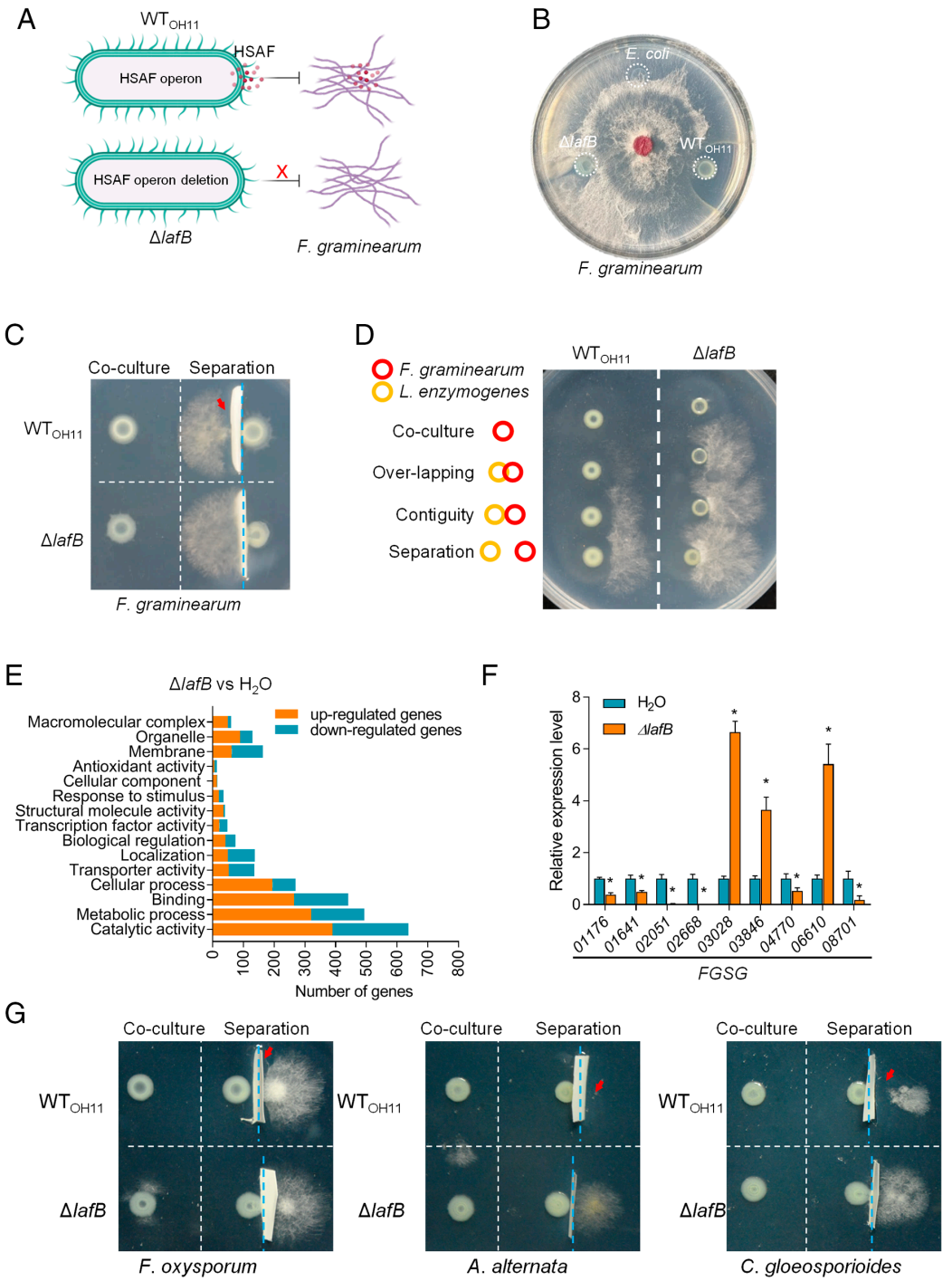

Fig. 1. Discovery of contact-dependent inhibition of filamentous fungal growth by *L. enzymogenes* OH11 independent of antifungal antibiotics. (*A*) *L. enzymogenes* OH11 secretes HSAF to inhibit *F. graminearum* PH-1. The *lafB* gene is critical for HSAF biosynthesis, with red dots indicating HSAF secretion by OH11. (*B*) The HSAF-defective mutant Δ*lafB* exhibited a nearly complete loss of antagonistic activity against PH-1. Bacterial strains were cultured in 10% TSB media to induce HSAF production, which was subsequently tested for antagonistic activity on 10% TSA plates. (*C*) *L. enzymogenes* inhibited conidial germination of *F. graminearum* PH-1 through a HSAF-independent and contact-dependent mechanism. Both the WT OH11 and Δ*lafB* hindered the growth of PH-1. Filter separation impeded cell-to-cell contact, resulting in diminished antifungal activity of Δ*lafB*, while WT OH11 displayed a small zone of inhibition outside the filter. Again, *L. enzymogenes* strains were cultured in 10% TSB media to induce HSAF production for antagonistic testing on 10% TSA. The blue dotted lines indicate the 0.22-μM PVDF filter, while the red arrows point to the inhibition zones. (*D*) WT OH11 inhibited PH-1 growth prior to cell contact, whereas Δ*lafB* did not. Red circles denote PH-1, while yellow circles represent *L. enzymogenes*. PH-1 and *L. enzymogenes* were inoculated at varying distance marked by circles. Bacteria cells suspended in water were inoculated onto PDA media to evaluate antifungal activity. (*E*) The number of differentially expressed genes (DEGs) categorized into various GO terms is illustrated. Orange columns represent up-regulated genes, while blue columns denote down-regulated genes. (*F*) Expression levels of selected genes were validated by qRT-PCR. Three replicates of each sample were analyzed with a *t* test. Asterisks indicate significant differences ($P < 0.01$). (*G*) *L. enzymogenes* strains inhibited growth of multiple filamentous fungi in a contact-dependent manner. Both WT OH11 and Δ*lafB* inhibited growth of *F. oxysporum*, *A. alternata,* and *C. gloeosporioides*, while filter separation obstructed cell-to-cell contact, thereby hindering antifungal activity of Δ*lafB*. Red arrows indicate zones of inhibition, and blue dotted lines depict the 0.22-μM PVDF filters.

However, when the intercellular contacts between bacterial cells and fungal conidia were separated by a 0.22-μM filter membrane, Δ*lafB* lost its antifungal activity, while WT OH11 maintained inhibition of fungal growth outside the membrane (Fig. 1*G*). Collectively, these findings suggest that the observed antifungal effects of *L. enzymogenes* through HSAF-independent intercellular contacts represent a common occurrence.

T6SS Is Required for Fungal Growth Inhibition Triggered by Intercellular Contacts. In the following context, we aim to elucidate the mechanisms by which *L. enzymogenes* achieves HSAF-independent antifungal effects through interkingdom intercellular contact, focusing specifically on the T6SS. This system not only mediates competition among bacterial species but also exhibits the capacity to kill yeast-like fungi (16, 17). Our previous work indicated that the genome of OH11 encodes a complete T6SS gene cluster and that the structural gene *tssM* is essential for the translocation of the inner-tube Hcp into the extracellular environment (28). To investigate the role of T6SS in *L. enzymogenes*'s antifungal activity independent of HSAF, we generated a double mutant, Δ*lafB*Δ*tssM*, by knocking out *tssM* in an HSAF-deficient mutant background (Δ*lafB*). We conducted coculture experiments on PDA plates using *L. enzymogenes* cells and conidia from four filamentous fungal pathogens- *F. graminearum*, *F. oxysporum*, *A. alternata,* and *C. gloeosporioides*. The results demonstrated that the Δ*lafB* mutant was largely unable to inhibit fungal growth in the absence of T6SS, whereas complementation with T6SS rescued this inhibitory effect (Fig. 2*A*). These findings strongly suggest that T6SS serves as the primary contact-dependent antifungal weapon employed by *L. enzymogenes* against filamentous fungi, independently of HSAF.

To assess the ecological significance of T6SS in enhancing plant protection against fungal infections by *L. enzymogenes* in the absence of HSAF, we conducted assays that involved mixing OH11 and related mutants with hyphal plugs of *F. graminearum*, followed by inoculating the mixtures on soybean leaves. Both OH11 and Δ*lafB* demonstrated significant inhibition of *F. graminearum* infection; however, the biocontrol activity of the Δ*lafB*Δ*tssM* double mutant was notably diminished (Fig. 2 *B* and *C*). Additionally, we inoculated *L. enzymogenes* cells on the surface of fungal-colonized seeds to establish a contact-dependent microenvironment. Treatments with WT OH11 and Δ*lafB* proved highly effective in protecting *Rhizopus*-contaminated watermelon (*Citrullus lanatus*) seeds from fungal infection, as evidenced by the absence of fungal mycelia on the seed surface (*SI Appendix*, Fig. S4). In contrast, the inactivation of T6SS in Δ*lafB* significantly impaired the protective capacity of *L. enzymogenes* (*SI Appendix*, Fig. S4). These plant assays collectively indicate that *L. enzymogenes* possesses an HSAF-independent antifungal strategy against filamentous fungal pathogens, with T6SS being a crucial contact-dependent weapon.

To evaluate whether *L. enzymogenes* can inhibit fungi in soil via T6SS, we mixed *F. graminearum* conidia with cultures of *L. enzymogenes* strains and inoculated the mixtures into sterile soil. After 7 d of incubation, we quantified the relative biomass of *F. graminearum* and *L. enzymogenes* using qPCR on total soil DNA. The result revealed a significant increase in the relative biomass of *F. graminearum* when T6SS was inactivated in *L. enzymogenes* (Fig. 2*D*). We also inoculated Δ*lafB* and Δ*lafB*Δ*tssM* into the naturally banana-planting soil to examine whether *L. enzymogenes* influences the soil fungal microbiome. The total fungal biomass decreased in soil treated by Δ*lafB*, while an increase was observed in soils treated by Δ*lafB*Δ*tssM* (Fig. 2*E*). Microbiome sequencing and PCoA confirmed that fungal communities from Δ*lafB*-treated soil were distinct from those derived from the soil treated by LB and the Δ*lafB*Δ*tssM* double mutant (Fig. 2*F*), indicating that *L. enzymogenes* can shape the fungal community in field settings through T6SS.

To further investigate the role of T6SS in the fungal inhibition by *L. enzymogenes*, we performed microscopy on *F. graminearum* PH-1. While WT OH11 did not inhibit the germination of *F. graminearum* conidia during the initial 8 h of coculture (*SI Appendix*, Fig. S5), conidia degradation was observed after 24 h, a result not achieved by Δ*lafB* or Δ*lafB*Δ*tssM* (*SI Appendix*, Fig. S5). Microscopic observations indicated that the elongation of germinating hyphae of *F. graminearum* was inhibited by Δ*lafB*, with this inhibitory effect markedly reduced in Δ*lafB*Δ*tssM* (Fig. 3 *A* and *B*). Scanning electron microscope (SEM) revealed that Δ*lafB* could make contact with the *F. graminearum* surface and induce partial hyphal degradation, whereas Δ*lafB*Δ*tssM* failed to elicit those effects (Fig. 3*C*). Further analysis through transmission electronic microscope (TEM) revealed deformation of the *F. graminearum* cell wall and plasma membrane upon contacting with Δ*lafB*, while cell deformity in Δ*lafB*Δ*tssM*-treated *F. graminearum* was partially restored (Fig. 3*D*). Chitin distribution was concentrated at the tips and septa of *F. graminearum* hyphae treated with ΔlafB, indicating that Δ*lafB* did not affect the polarized growth of *F. graminearum* germinating hyphae (*SI Appendix*, Fig. S5). Under poor nutrient conditions (such as 10% TSB), HSAF generation is up-regulated, while T6SS assembly occurs under rich nutrient conditions (such as LB) (28). Interestingly, while HSAF disrupts polarized growth of fungi (21, 24), intercellular contact-dependent fungal inhibition by *L. enzymogenes* is accomplished through alternative mechanisms, further supporting that this fungal inhibition is independent of HSAF.

We analyzed the comparative transcriptomes of *F. graminearum* PH-1 conidia treated with Δ*lafB* and the double mutant Δ*lafB*Δ*tssM* to identify fungal genes significantly affected upon contact with *L. enzymogenes* cells. In the Δ*lafB*Δ*tssM* treatment group, 648 genes were up-regulated and 431 down-regulated compared to the Δ*lafB* treatment (*SI Appendix*, Fig. S6 and Dataset S1). The GO enrichment analysis showed similar patterns of DEGs in Δ*lafB*-treated samples when compared to the control; however, T6SS deficiency did not alter the expression of any genes involved in antioxidant activity (Fig. 3*E*). These results suggest that the contact-dependent inhibition of fungal growth from conidia to hypha by *L. enzymogenes* is primarily mediated through T6SS, although other oxidative stress-inducing mechanisms may also play a role. Additionally, we found 87 genes related to cell membrane processes that were differentially expressed. KEGG annotation revealed that five fungal genes associated with glycerophospholipid metabolism and fungal membrane biogenesis were down-regulated in Δ*lafB*Δ*tssM*-treated fungi, whereas expression levels were elevated in fungi treated with Δ*lafB* (*SI Appendix*, Fig. S6). These results imply that the T6SS of *L. enzymogenes* potentially disrupts the cell structure of *F. graminearum*, supporting the findings from both SEM and TEM assays (Fig. 3 *C* and *D*). The expression levels of selected genes involved in the conidia production and germination regulation were validated by qRT-PCR, including *FGSG_09031* (oxysterol binding protein, indispensable for ergosterol biosynthesis), *FGSG_03946* (thioredoxin), *FGSG_01763* (hydrophobin) (29–31) (Fig. 3*F*). These results further indicate that the T6SS of *L. enzymogenes* may exert its antifungal effects by directly or indirectly disrupting the properties of fungal cell structure.

The T6SS Effector Le1893 Demonstrated Antifungal Activity When Expressed in Yeast. Given that the T6SS has been shown to translocate yeast-killing toxic effectors, our objective was to

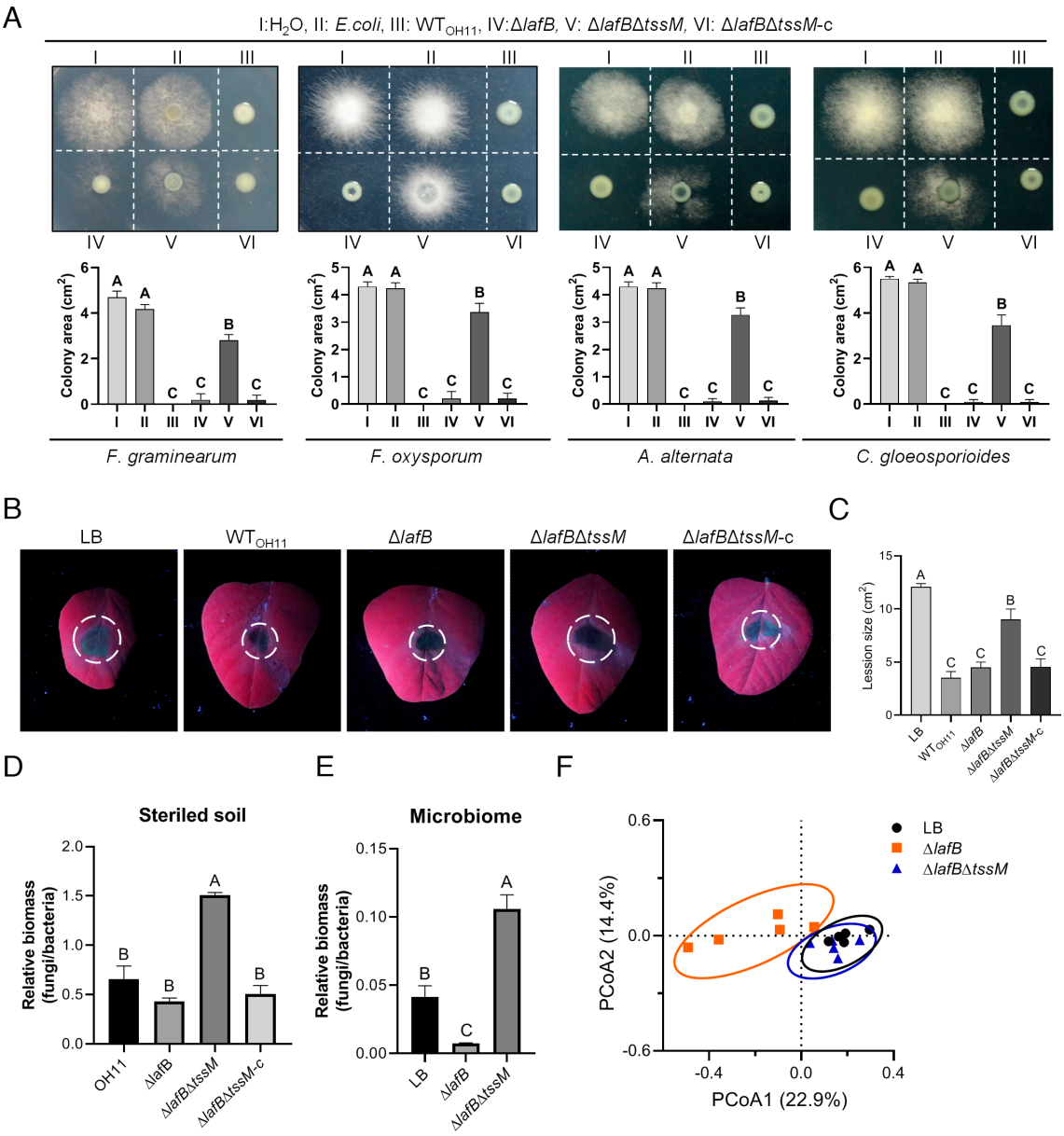

Fig. 2. T6SS is essential for contact-dependent inhibition of fungi by *L. enzymogenes*. (*A*) T6SS is critical for the contact-dependent inhibition of various filamentous fungi by *L. enzymogenes* without HSAF. Δ*lafB*Δ*tssM* exhibited significantly reduced inhibitory activity against all tested fungi compared with Δ*lafB*, whereas the *tssM* complementation strain Δ*lafB*Δ*tssM*-c restored this defect. Bacteria cells suspended in water were inoculated onto PDA media to assess antifungal activity. The down panels were fungal colony sizes quantified from the upper panels. Three replicates of each sample were analyzed using a one-way ANOVA, and different letters indicated the significant differences ($P < 0.01$). (*B*) *L. enzymogenes* prevents soybean infection by *F. graminearum* through T6SS. Hyphal plugs of *F. graminearum* were combined with culture of *L. enzymogenes*–related strains. After coculturing for 1 h, the hyphal plugs were inoculated onto soybean leaves for 2 d, and images were captured under UV light. (*C*) Quantification of lesion sizes in panel *B*. Three replicates of each sample were analyzed with a one-way ANOVA test. Different letters indicate the significant differences ($P < 0.01$). (*D*) The relative biomass of *F. graminearum* significantly increased during interactions with Δ*lafB*Δ*tssM* in soil. Conidia of *F. graminearum* were mixed with *L. enzymogenes* strains and subsequently inoculated into sterile soil, which was cultured for 7 d. The relative biomass of *F. graminearum* and *L. enzymogenes* was measured by qPCR using total soil DNA. Three replicates of each sample were analyzed with a one-way ANOVA test. Different letters indicate the significant differences ($P < 0.01$). (*E*) *L. enzymogenes* inhibited fungal biomass in natural soil via T6SS. Strains Δ*lafB* and Δ*lafB*Δ*tssM* were individually inoculated into the natural soil planted with banana for 7 d. The relative biomass of total fungi and bacteria was measured by qPCR using total soil DNA, with three replicates of each sample analyzed with a one-way ANOVA, and different letters indicating the significant differences ($P < 0.01$). (*F*) Principal coordinates analysis (PCoA) of microbiome sequencing indicated that the fungal communities derived from the Δ*lafB*-treated soil were clustered separately from those derived from the LB-treated soil and the Δ*lafB*Δ*tssM*-treated soil.

identify such effectors in *L. enzymongenes* using yeast as our working model, owing to its well-established heterogeneous gene-induction system (32). We first assessed whether *L. enzymogenes* also employs T6SS to target yeast by coculturing mCherry-labeled Δ*lafB* cells and GFP-labeled *Saccharomyces cerevisiae* (W303) cells (OD_{600} = 1.0) at a 1:1 volume ratio on YPD agar plates. No GFP signal was observed; however, separating the bacterial and yeast cells using a 0.22-μM filter allowed for simultaneous detection of GFP and mCherry signals (Fig. 4*A*). During this process, T6SS appeared to play a key role, as the blockade of T6SS by the *tssM* mutation in Δ*lafB* reduced its antifungal activity against yeast growth, as evidenced by fluorescent microscopy and viable yeast cell counts (Fig. 4 *B* and *C*). Proteins containing PAAR domains are among the most well-studied effectors of bacterial T6SS translocation (33). We searched the genome of OH11 and identified three proteins containing PAAR domain (Le1893, Le2217, and Le4961) (*SI Appendix*, Fig. S7). The artificial expression of these three predicted PAAR domain-containing proteins in *S. cerevisiae*

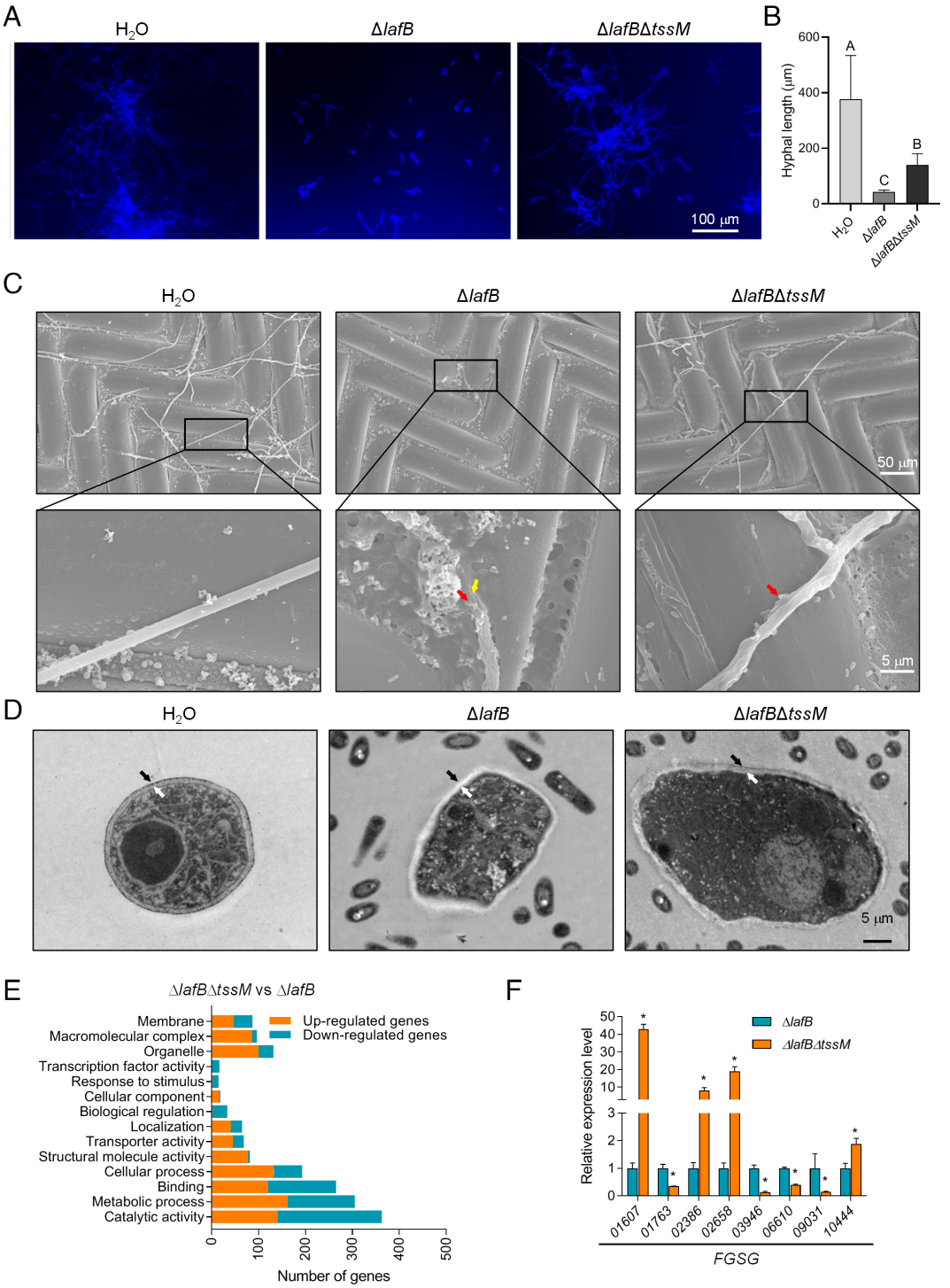

Fig. 3. *L. enzymogenes* inhibits the elongation of germinating hyphae of *F. graminearum* through T6SS. (*A*) Elongation of *F. graminearum* PH-1 germinating hyphae was inhibited by Δ*lafB*, whereas the inhibitory capacity of Δ*lafB*Δ*tssM* was significantly diminished. The hyphae were stained by CFW to enhance visibility. (*B*) Quantification of hyphae length from panel *A*. Three replicates of each sample were analyzed with a one-way ANOVA test. Different letters indicate the significant differences ($P < 0.01$). (*C*) SEM analysis demonstrated that Δ*lafB* resulted in partial hyphal degradation of strain PH-1, while this defect was less pronounced in the Δ*lafB*Δ*tssM* double mutant. Red arrows indicate the attachment of *L. enzymogenes* cells to *F. graminearum* hypha. Yellow arrows indicate *F. graminearum* hypha was partially degraded. (*D*) Transmission electron microscopy analysis demonstrated that Δ*lafB* caused deformations in the cell wall and plasma membrane of strain PH-1, while these deformations were partially restored during interactions with Δ*lafB*Δ*tssM*. Black arrows indicate cell wall, and white arrows indicate cell membrane. (*E*) The number of DEGs categorized into various GO terms. Orange spots indicate up-regulated genes, while blue spots denote down-regulated genes. (*F*) Expression levels of selected genes were assessed by qRT-PCR. Three replicates of each sample were analyzed with a *t* test. Asterisks indicate the significant differences ($P < 0.01$).

revealed that one of them (Le1893) exhibited antifungal activity against yeast (*SI Appendix*, Fig. S7). Additionally, when 3 VgrG proteins, often acting as the syringe components of T6SS (13), were expressed in *S. cerevisiae*, none was found to inhibit yeast growth (*SI Appendix*, Fig. S7).

By searching in the conserved domain database (34), we determined that Le1893 contained a PAAR domain, a Rearrangement Hot Spot (RHS) ligand-binding domain, and an AHH nuclease superfamily domain. We utilized Alphafold2 to predict the structure of Le1893 (35), and found that its structure was similar to

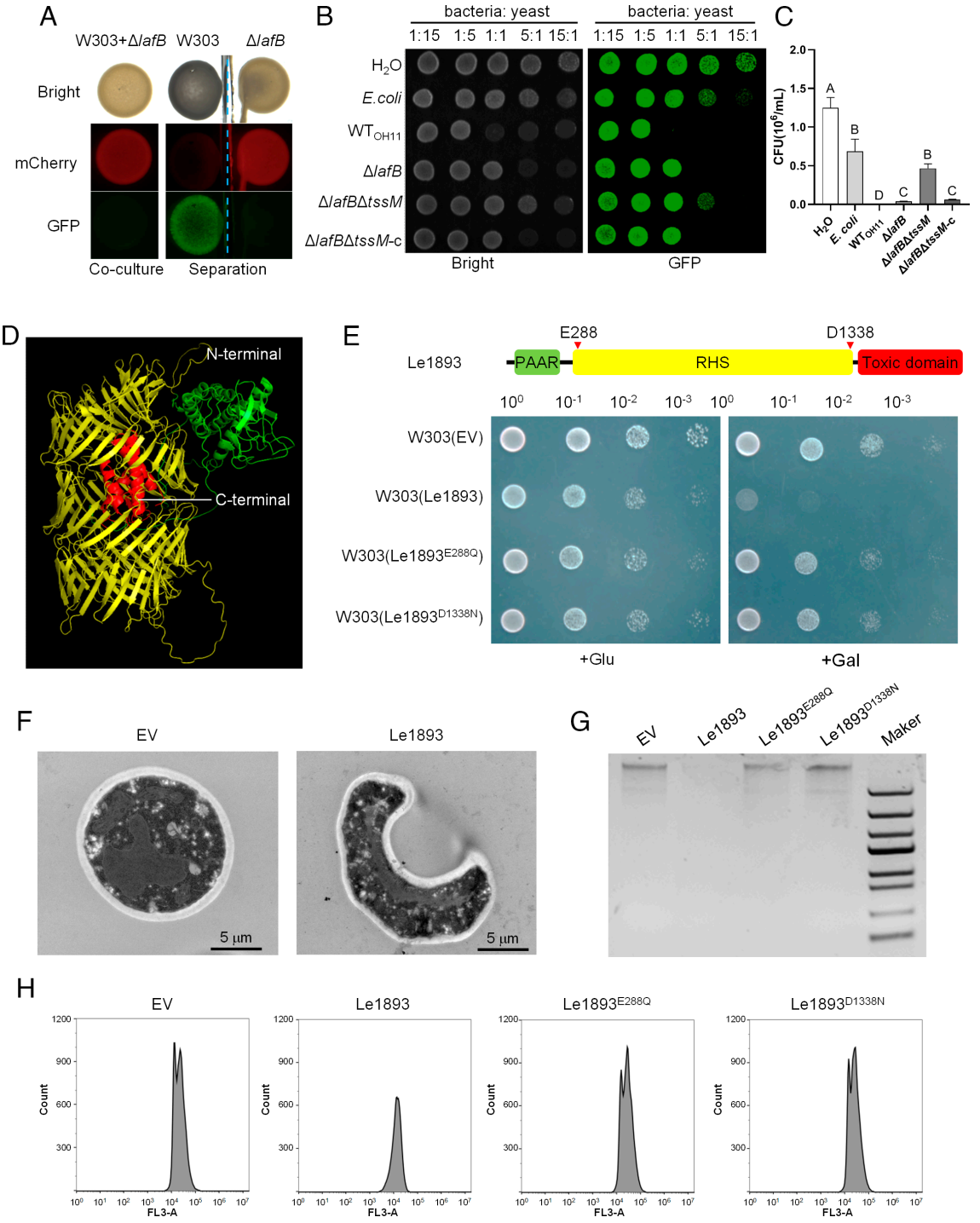

Fig. 4. The *L. enzymogenes* T6SS effector Le1893 demonstrates antifungal activity. (*A*) *L. enzymogenes* inhibited yeast growth in a manner that was both HSAF-independent and dependent on cell-to-cell contacts. The HSAF-defective mutant Δ*lafB*(mCherry) inhibited the growth of yeast strain W303(GFP) after coculturing for 24 h. Blocking of intercellular contact with a filter resulted in a loss of antifungal activity. The blue dotted line represented the 0.22-μM PVDF filter. Bacterial cells suspended in water were inoculated onto YPD media to assess their antifungal activity. (*B*) Δ*lafB*Δ*tssM* exhibited reduced antifungal activity against yeast. Normalized bacterial strains and yeast strain W303(GFP) were mixed in various volumetric ratios and cultured for 24 h prior to analysis. (*C*) The living number of CFU of W303 (bacteria: yeast = 5:1) in panel *B* was quantified. Three replicates of each sample were analyzed using a one-way ANOVA test. Different letters indicate the significant differences ($P < 0.01$). (*D*) The structure of Le1893 was predicted by AlphaFold2. Color codes: PAAR domain (green), RHS domain (yellow), C-terminal toxin domain (red). (*E*) Mutation of the predicted self-cleavage sites in Le1893 resulted in the loss of antifungal activity. W303-derived yeast strains were diluted to a series of ODs and cultured for 48 h on either noninducing (glucose) or inducing (galactose) media. (*F*) Transmission electron microscopy observation revealed that Le1893 induced deformation of yeast cells. (*G*) The abundance of genomic DNA was significantly reduced in the yeast strain expressing Le1893, whereas strains expressing the mutants of self-cleavage site did not affect genomic DNA abundance. The W303 strains were cultured in SC-U medium supplemented with 2% galactose for 12 h. 1×10^6 yeast cells were harvested and the DNA contents were evaluated through genomic DNA isolation. (*H*) Flow cytometer analysis demonstrated that Le1893 decreased DNA concentration in yeast cells, while strains expressing the mutated self-cleavage site did not achieve a similar reduction. The W303 strains were cultured in SC-U medium supplemented with 2% galactose for 12 h. 1×10^6 yeast cells were stained by propidium iodide, and then the DNA content was quantified using flow cytometry. FL3-A indicated the fluorescence signal detected by flow cytometry.

that of RHS family toxins (Fig. 4*D*). RHS toxins typically consist of an N-terminal region responsible for secretion, a conserved middle shell-like region, and a variable C-terminal toxic region (36). Sequence alignment with RHS toxins led us to predict two self-cleavage sites essential for the release of the toxic region of Le1893 (*SI Appendix*, Fig. S7). Upon individual mutation of these cleavage sites, the resultant mutants lost lethal effects on yeast cells (Fig. 4*E*), supporting that Le1893 is an RHS-like toxin. TEM observations indicated that the expression of Le1893 resulted in deformities in yeast cells (Fig. 4*F*). The C-terminal structure of Le1893 differed from that of homologous RHS proteins and belonged to the AHH nuclease superfamily domain. To investigate whether Le1893 impedes fungal growth by degrading fungal DNA, we extracted the genomic DNA from yeast expressing Le1893 and the site-mutated variants. The result demonstrated that Le1893 reduced the genomic DNA abundance in yeast, while the self-cleavage site mutants lost this function (Fig. 4*G*). This result was corroborated by flow cytometer analysis (Fig. 4*H*). Although we did not observe Le1893-induced DNA degradation in yeast cells (Fig. 4*G*), we propose that Le1893 exerts its antifungal activity by influencing the total DNA content. Furthermore, we knocked out *Le1893* in the Δ*lafB* background and determined that it was not essential for the contact-dependent antifungal activity of Δ*lafB*, indicating that Le1893 is not the sole T6SS antifungal effector encoded by *L. enzymogenes* (*SI Appendix*, Fig. S8).

The T6SS-Mediated Antibiotics-Independent Antifungal Mode Was Also Present in *Pseudomonas fluorescens*. We examined whether other representative beneficial soil bacteria target filamentous fungi in a manner similar to *L. enzymogenes.* We selected six additional laboratory strains, including *Lysobacter antibioticus* OH13, *Lysobacter brunescens* OH21, *P. fluorescens* 2P24 and Pf0-1, and *Pseudomonas protegens* Pf-5 and CHA0. Cells from each tested strain were mixed with conidia of *F. graminearum* PH-1 and coinoculated on PDA agar plates. The results indicated that only *P. fluorescens* 2P24 effectively inhibited the transition from conidia to hyphae (Fig. 5*A*). To test whether this antifungal activity exhibited by *P. fluorescens* is independent of antifungal metabolites, we took into consideration that *P. fluorescens* 2P24 produces 2,4-DAPG as its primary antifungal antibiotic (37) (Fig. 5*B*). We utilized a specific 2,4-DAPG-deficient mutant Δ*phl*, in which the entire *phl* gene cluster responsible for 2,4-DAPG biosynthesis was knocked out (37). As depicted in Fig. 5*C*, the mutant almost exhibited a significant loss of antagonistic activity against the *F. graminearum* PH-1 mycelium on PDA plates. However, coculturing its cells with PH-1 conidia still resulted in fungal inhibition (Fig. 5*D*). Separation of bacterial cells from PH-1 conidia via a 0.22-μM filter led to the observed loss of antifungal activity in Δ*phl*, while the WT 2P24 remained effective (Fig. 5*D*). Subsequently, we generated a 2,4-DAPG and T6SS double-deficient mutant (Δ*phl*Δ*hcp*) by knocking out *hcp* in the Δ*phl* background. Δ*phl*Δ*hcp* showed reduced antifungal activity compared to Δ*phl* via a contact-dependent antifungal assay (Fig. 5 *E* and *F*). This functional defect in Δ*phl*Δ*hcp* was rescued by *hcp* complementation via a chromosomal knock-in approach (Fig. 5 *E* and *F*), indicating that *P. fluorescens* T6SS plays a role in contact-dependent antifungal effects. Furthermore, we observed cell-to-cell interactions between *P. fluorescens* and *F. graminearum* at various time points using microscopy. We found that WT 2P24, Δ*phl,* and Δ*phl*Δ*hcp* were unable to inhibit the germination of PH-1 conidia during the early stage (8 h) of coculture (*SI Appendix*, Fig. S9). After 24 h of coculture, we observed that Δ*phl* could partially inhibit the elongation of germinating PH-1 hypha, but this ability was diminished in Δ*phl*Δ*hcp* (*SI Appendix*, Fig. S9). Collectively, these results suggest that T6SS-mediated contact-dependent antifungal activity is also present in *P. fluorescens*, another prevalent bacterial species within the soil microbiome.

Antibiotics-Independent Fungal Inhibition Triggered by Intercellular Contact Naturally Occurs Within the Soil Microbiome. Given the widespread presence of *Lysobacter* and *Pseudomonas* strains across various natural ecological niches, particularly in the belowground compartments of plants, we investigated whether naturally occurring soil-borne bacteria can inhibit fungal growth from conidia to hyphae. We isolated soil bacteria that inhabit the same ecological niche as fungi using a modified conidia enrichment approach based on previous work conducted in our laboratory (38). Soil samples were collected from soybean fields and diluted with sterilized ddH_2O. These diluted soil samples were then mixed with conidia of soybean root rot pathogen *F. oxysporum*. The resulting mixtures were incubated for 24 h, filtered through a 0.45-μM filter, and washed with sterilized ddH_2O to remove nonspecifically adsorbed bacteria. Following this, the mixtures were diluted and smeared onto PDA plates. We hypothesized that during coincubation, bacteria exhibiting contact-dependent activity against *F. oxysporum* in soybean fields would accumulate around the fungi. Indeed, both *F. oxysporum* and bacterial colonies appeared on the plate after 48 h, and single bacterial colonies near *F. oxysporum* colonies were subsequently picked (*SI Appendix*, Fig. S10). Using this approach, we identified 14 distinct bacterial isolates, designated "FoE1" (F. *oxysporum* Enriched strain 1) through "FoE14", from soybean field. Antagonistic assays, conducted without intercellular contact, revealed that one isolate, FoE4, demonstrated a significant zone of inhibition against *F. oxysporum*, while FoE13 exhibited slight antagonistic activity. The remaining 12 strains did not display antagonistic effects under comparable conditions (*SI Appendix*, Fig. S10). Coculturing bacterial cells with *F. oxysporum* conidia revealed that four isolates (FoE4, FoE5, FoE9, and FoE13) inhibited the growth of *F. oxysporum* from conidia to hyphae (*SI Appendix*, Fig. S10). Sequencing analysis of 16S rRNA fragment determined that FoE4 and FoE9 were identified as *Pseudomonas* species, while FoE5 and FoE13 were assigned to the genera *Bacillus* and *Pantoea*, respectively (*SI Appendix*, Fig. S10). We then employed membrane separation to investigate whether these four isolates possessed contact-dependent antifungal weapons. Separation of bacterial and fungal growth using filters indicated that FoE5, FoE9, and FoE13 lost their antifungal activity (Fig. 5*G*); however, the antifungal activity of *Pseudomonas* FoE4 remained unaffected by membrane separation (Fig. 5*G*), suggesting that FoE4 primarily inhibited fungal growth through the production of antifungal metabolites. We could not conclusively determine whether antifungal activity of FoE13 depended on intercellular contact. The comparison of the antagonistic and contact-dependent assays led us to propose that isolates FoE5 and FoE9 may inhibit fungal growth in an intercellular contact-dependent manner.

Subsequently, we conducted plant growth assays using isolates FoE4, FoE5, and FoE9 with watermelon seeds. FoE5 and FoE9 demonstrated efficacy in protecting watermelon seeds from fungal infection, comparable to the control (FoE4), which produced an antifungal metabolite, as no fungal mycelium was observed on the seed surface (*SI Appendix*, Fig. S11). Furthermore, FoE5 and FoE9, in contrast to FoE4, promoted germination of watermelon seeds (*SI Appendix*, Fig. S11), suggesting these isolates may also enhance plant growth. These results corroborate that the conidia enrichment method was effective for identifying

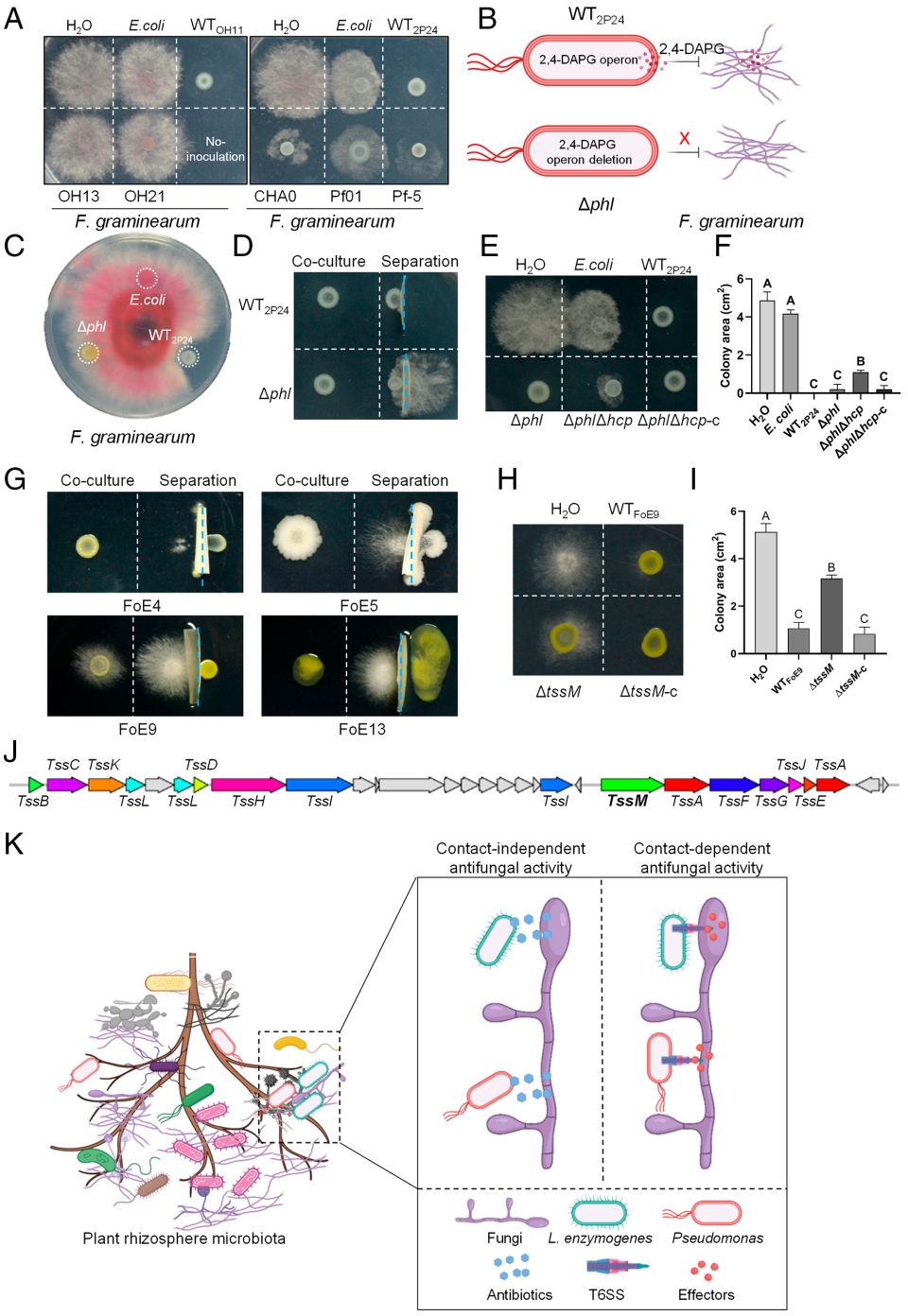

Fig. 5. *Pseudomonas* strains 2P24 and FoE9 inhibit the growth of *Fusarium* in a contact-dependent manner mediated by T6SS. (*A*) *P. fluorescens* 2P24 demonstrated growth inhibition of *F. graminearum* PH-1. *Lysobacter* strains and *Pseudomonas* strains were cocultured with PH-1 for 48 h, respectively. OH13 is *L. antibioticus*; OH21 is *L. brunescens*; Pf01 is *P. fluorescens*; Pf-5 and CHA0 are *P. protegens*. Bacteria cells suspended in water were inoculated onto PDA media to assess antifungal activity. (*B*) *P. fluorescens* 2P24 secreted 2,4-diacetylphloroglucinol (2,4-DAPG) to inhibit *F. graminearum* PH-1, with the *phl* gene cluster being essential for 2,4-DAPG biosynthesis. (*C*) The 2,4-DAPG biosynthesis-defective mutant Δ*phl* exhibited a loss of antagonistic activity against PH-1 compared to WT 2P24. Bacterial strains were cultured in LB media containing 2% glucose to induce 2,4-DAPG biosynthesis, after which the cultures were inoculated onto PDA media to evaluate antifungal activity. (*D*) *P. fluorescens* 2P24 inhibited the growth of PH-1 in a contact-dependent manner independent of 2,4-DAPG. Filter separation impeded intercellular contact, resulting in hindered antifungal activity of Δ*phl*, but not WT 2P24. The blue dotted lines denote the 0.22-μM PVDF filter. Bacterial strains were cultured in LB media containing 2% glucose prior to being inoculated onto PDA media for antifungal testing. (*E*) The Δ*phl*Δ*hcp* double mutant exhibited decreased antifungal activity compared to Δ*phl*; however, the *hcp* complementation strain Δ*phl*Δ*hcp*-c restored this defect. Bacteria cells, suspended in water, were inoculated onto PDA media to test antifungal activity. (*F*) Fungal colony sizes quantified from panel *E*. Three replicates of each sample were analyzed with a one-way ANOVA test. Different letters indicate the significant differences ($P < 0.01$). (*G*) The obstruction of intercellular contacts by filter separation resulted in hindered antifungal activity of FoE5, FoE9, and FoE13. The blue dotted lines indicate the 0.22-μM PVDF filter, with FoE4 and FoE9 cultured in LB plus 2% glucose media, while FoE5 and FoE13 were sustained in LB media. Cultures were then inoculated onto PDA media for antifungal assessment. (*H*) Mutation of *tssM* in FoE9 led to a partial reduction in antifungal activity on PDA media. (*I*) Fungal colony sizes quantified from panel *H*. Three replicates of each sample were analyzed with a one-way ANOVA test. Different letters indicate the significant differences ($P < 0.01$). (*J*) A T6SS gene cluster was identified in the genome of FoE9. (*K*) The working model depicts contact-dependent and contact-independent antifungal activities of bacteria. In the soil ecosystem, beneficial bacteria such as *L. enzymogenes* OH11 and *P. fluorescence* 2P24 secreted antibiotics to inhibit fungi in a contact-independent manner. Conversely, strains OH11, 2P24, and other soil microbiome bacteria, including FoE5 and FoE9, can also inhibit filamentous fungi through contact-dependent mechanisms, even in the absence of antibiotic metabolites. In the cases of strains OH11, 2P24, and FoE9, T6SS plays a crucial role in this contact-dependent antifungal activity, potentially by translocating T6SS effectors into fungal cells.

natural soil bacteria exhibiting intercellular contact-triggered antifungal activity. In support, we found that neither FoE5 nor FoE9 inhibited conidia germination at an early stage (8 h) during the coculture of bacterial cells and fungal conidia (*SI Appendix*, Fig. S11), while *F. oxysporum* hyphal elongation was inhibited by both FoE5 and FoE9 after 24 h of coculture (*SI Appendix*, Fig. S11). Collectively, these observations suggest that intercellular contact-triggered antifungal activity occurs naturally within the soil microbiome, as represented by FoE5 and FoE9. To further substantiate these findings, we sequenced the genome of FoE9 and confirmed the presence of a T6SS gene cluster (Fig. 5*J*). Subsequent to the knockout of the *tssM* gene in FoE9, we observed a partial reduction in the antifungal activity of the mutant, indicating that T6SS is involved in the contact-dependent antifungal activity of FoE9 (Fig. 5 *H* and *I*).

Discussion

Diffusible antibiotic metabolites have traditionally been viewed as a primary strategy for bacteria to compete with fungi counterparts in natural ecosystems. Contrary to the prevailing belief that bacteria inhibit fungi mainly through the production of these metabolites, we have identified an antifungal phenomenon that operates independently of antibiotic metabolites, relying instead on intercellular contacts between bacterial cells and fungal conidia. This mode of fungal inhibition holds significant ecological and biological implications for protecting plants from fungal infection and appears to be naturally occurring in the soil microbiome (Fig. 5*J*). Our findings thus added a dimension to the understanding of BFIs within the soil microbiome, demonstrating that soil bacteria can inhibit filamentous fungi not only by secreting antifungal metabolites but also through intercellular contact via the T6SS (Fig. 5*J*).

Previous studies have indicated that the T6SS produced by bacterial pathogens can target yeast-like fungi such as *S. cerevisiae* and the human pathogen *Candida* (16, 17). Some bacterial T6SS effector proteins also showed in vitro antifungal activity to filamentous fungi (39). In contrast, this study expands the role of T6SS to include contact-dependent inhibition of phytopathogenic filamentous fungi by soil-borne plant-beneficial bacteria. Given that almost all fungal diseases in the field of crop protection are caused by filamentous fungi, we propose that T6SS-mediated interactions between bacteria and filamentous fungi could offer an approach for controlling crop fungal diseases.

As previously noted, bacteria can engage in multiple interaction modes with biologically and ecologically significant fungi (3, 40). Among these, diffusible chemicals represent a predominant mode of BFI. In this context, chemicals secreted by donor cells diffuse into the environment, where they can act as antibiotics or signaling molecules influencing the physiology of recipient cells. These chemically mediated BFIs do not rely on direct intercellular contact between bacteria and fungi (40, 41). Beyond this dominant mode, bacteria may also adhere to fungal surfaces or invade fungal cells through physical intercellular interactions (42). Such cell-to-cell interactions facilitate cooperation between symbiotic bacteria and fungi, enhancing their survival and pathogenesis. For instance, *Serratia proteamaculans* attaches to the surface of *Mucor lanceolatus* hypha, using the fungus as a scaffold for attachment and movement (43). *Mycetohabitans rhizoxinica* invades *Rhizopus microconidia* cells and persists as an endophyte. Moreover, the rhizoxin produced by *M. rhizoxinica* is crucial for the pathogenesis of *R. microconidia* (44). Therefore, the intercellular contact-mediated growth inhibition of filamentous fungi by antibiotic metabolite-independent soil bacteria identified in our study represents a unique BFI pattern with distinct ecological significance in the soil microbiome. This cross-kingdom interaction between soil bacteria and fungi may provide critical insights into the complexity of microbial communities.

The finding of T6SS-mediated growth inhibition of filamentous fungi by soil bacteria broadens the known efficacy of T6SS. As a widely recognized contact-dependent lethal mechanism, T6SS is primarily thought to target and eliminate gram-negative bacteria during interspecies interactions (45). Additionally, T6SS and its effectors have also been reported to act against gram-positive bacteria (45). Beyond its antibacterial capabilities, T6SS displays anti-eukaryotic-cell activity as well. Numerous pathogenic and beneficial bacteria translocate toxic T6SS effectors to target their eukaryotic host cells (46). For instances, the T6SS and its effectors of the plant beneficial bacterium *P. protegens* CHA0 are implicated in the killing of *Pieris brassicae* (47). T6SS also targets and disrupts yeast-like fungi by delivering toxic effectors (16, 17). In this study, we demonstrate that *L. enzymogenes*, a soil-borne bacterium, protects plants from filamentous fungal infections through T6SS-mediated intercellular interactions. Specifically, this bacterium likely cross-translocates the RHS family toxin effector Le1893, which has the potential to impact fungal DNA contents. Our findings indicate that T6SS was responsible for the contact-dependent inhibition of fungal genes associated with hypha development. These results suggest soil bacteria may develop antibiotic-independent, contact-dependent antifungal mechanisms. Supporting this hypothesis, we also present evidence that two other soil bacteria, *P. fluorescens* 2P24 and *P. fulva* FoE9, utilize T6SS as antifungal devices.

Our findings reveal a previously unidentified antifungal phenomenon associated with the predatory behavior of *L. enzymogenes*. In the soil microbiome, this bacterium coexists symbiotically with various filamentous fungi. Acting as a natural antifungal agent, *L. enzymogenes* can navigate toward nearby fungal hyphae or conidia via type IV pilus-driven twitching motility, subsequently attaching to these fungal structures (48). During migration, the bacterium produces and secretes a "long-range" antifungal compound, HSAF, which inhibits the growth of fungal hypha and the germination of conidia (49). Upon attachment to fungal cells, the bacterium generates a variety of lytic enzymes, including chitinase, β-1,3-glucanase, and protease to degrade fungal cells as a nutrient source (50). Our study indicates that when attached to fungal cells, particularly fungal conidia, *L. enzymogenes* can also activate the "short-range" antifungal apparatus known as T6SS to inhibit the growth of conidia into hyphae. This adaptation appears to facilitate predation of filamentous fungi, as the latter can escape *L. enzymogenes* through polarized hyphal growth when conidia differentiate into hypha. Furthermore, T6SS-mediated fungal inhibition sheds light on why *L. enzymogenes* possesses both T6SS and T4SS; T6SS is implicated in contact-dependent fungal inhibition, whereas T4SS is associated with contact-dependent bacterial killing. Supporting this conclusion, *L. antibioticus* OH13 and *L. brunescens* OH21 encode only the T4SS and lack the T6SS, which correlates their inability to mediate contact-dependent fungal inhibition. Notably, the Δ*lafB*Δ*tssM* strain exhibited residual antifungal activity (Fig. 2*A*), suggesting that alternative antifungal mechanisms, such as the flagellar type III secretion system (FT3SS), may also contribute to contact-dependent antifungal inhibition. This is supported by previous findings showing that FT3SS in *L. enzymogenes* facilitates the export of antifungal toxins (51).

In summary, we have elucidated that intercellular contact serves as a prevalent mode of interaction between beneficial soil bacteria and pathogenic filamentous fungi. Beneficial bacteria within the soil microbiome can effectively guard against pathogenic fungal infections through antibiotics-independent intercellular interactions mediated by the T6SS. These findings suggest that leveraging antibiotics-independent intercellular interactions could offer an alternative strategy for engineering the soil microbiota to mitigate plant fungal diseases, thereby reducing the risk of promoting antibiotic resistance in agricultural contexts.

Materials and Methods

Details of the *Materials and Methods* used in this study are provided in *SI Appendix, Materials and Methods*, and include strains and growth conditions, genetic approaches, contact-dependent antifungal assay, microscope observation, contact-independent antifungal assay, RNA-seq, transcriptome analysis, microbiome analysis, qRT-PCR assays, genome sequencing of FoE9, prediction of PAAR domain-containing proteins, antifungal activity assay of PAAR domain-containing proteins, propidium iodide staining and DNA content analysis, and isolation of antifungal bacteria based on enrichment of fungal pathogens.

Data, Materials, and Software Availability. The raw RNA sequencing data and microbiome data reported in this study have been deposited in the NCBI under the Accession No: PRJNA971132 (52) and PRJNA1158950 (53). The genome sequence of FoE9 was available in the NCBI GeneBank with Accession No: PRJNA1158498 (54). Additionally, the 16S rRNA sequences of FoE4, FoE5, FoE9, and FoE13 have been submitted to the NCBI GeneBank, with the corresponding accession numbers presented in *SI Appendix*, Fig. S10.

ACKNOWLEDGMENTS. We thank Dr. Xiaogang Wu (Guangxi University), Prof. Cong Jiang (Northwest A and F University), Prof. Zhonghua Ma (Zhejiang University), Dr. Hailei Wei (Chinese Academy of Agricultural Sciences), Dr. Ping Ma (Hebei Academy of Agriculture and Forestry Sciences), Prof. Yuanchao Wang (Nanjing Agricultural University), Prof. Huijun Wu (Nanjing Agricultural University), and Prof. Qin Gu (Nanjing Agricultural University) for providing bacteria and fungi strains used in this study. This work was financially supported by the National Natural Science Foundation of China (U22A20486, 32072470, and 32272619), the Fundamental Research Funds for the Central Universities (KJJQ2024014), Jiangsu Agricultural Sciences and Technology Innovation Fund [CX(18)1003], and Innovation Team Program for Jiangsu Universities (2017).

Author affiliations: [a]Department of Plant Pathology, Key Laboratory of Plant Immunity, Key Laboratory of Integrated Management of Crop Diseases and Pests, College of Plant Protection, Nanjing Agricultural University, Nanjing 210095, China; [b]Engineering Laboratory for Kiwifruit Industrial Technology, Key Laboratory of Plant Germplasm Enhancement and Specialty Agriculture, Wuhan Botanical Garden, Chinese Academy of Sciences, Wuhan 430074, China; [c]Department of Microbiology, Key Lab of Microbiology for Agricultural Environment, College of Life Sciences, Nanjing Agricultural University, Nanjing 210095, China; [d]State Key Laboratory of Rice Biology and Breeding, Ministry of Agricultural and Rural Affairs Laboratory of Molecular Biology of Crop Pathogens and Insects, Zhejiang University, Hangzhou 310058, China; and [e]Department of Plant Protection, Zhejiang Key Laboratory of Biology and Ecological Regulation of Crop Pathogens and Insects, Institute of Pesticide and Environmental Toxicology, College of Agriculture and Biotechnology, Zhejiang University, Hangzhou 310058, China

1. S. V. Avery, I. Singleton, N. Magan, G. H. Goldman, The fungal threat to global food security. *Fungal Biol.* **123**, 555–557 (2019).
2. M. C. Fisher, N. J. Hawkins, D. Sanglard, S. J. Gurr, Worldwide emergence of resistance to antifungal drugs challenges human health and food security. *Science* **360**, 739–742 (2018).
3. Y. Zhou *et al.*, Bacterial–fungal interactions under agricultural settings: From physical to chemical interactions. *Stress Biol.* **2**, 22 (2022).
4. C. Zhan, H. Matsumoto, Y. Liu, M. Wang, Pathways to engineering the phyllosphere microbiome for sustainable crop production. *Nat. Food* **3**, 997–1004 (2022).
5. D. Fira, I. Dimkic, T. Beric, J. Lozo, S. Stankovic, Biological control of plant pathogens by *Bacillus* species. *J. Biotechnol.* **285**, 44–55 (2018).
6. D. Haas, G. Defago, Biological control of soil-borne pathogens by fluorescent pseudomonads. *Nat. Rev. Microbiol.* **3**, 307–319 (2005).
7. J. M. Raaijmakers, I. De Bruijn, O. Nybroe, M. Ongena, Natural functions of lipopeptides from *Bacillus* and *Pseudomonas*: More than surfactants and antibiotics. *FEMS Microbiol. Rev.* **34**, 1037–1062 (2010).
8. X. Zhu *et al.*, Design, synthesis and biological activity of hydroxybenzoic acid ester conjugates of phenazine-1-carboxylic acid. *Chem. Cent. J.* **12**, 111 (2018).
9. S. Panthee, H. Hamamoto, A. Paudel, K. Sekimizu, *Lysobacter* species: A potential source of novel antibiotics. *Arch. Microbiol.* **198**, 839–845 (2016).
10. Y. Xie, S. Wright, Y. Shen, L. Du, Bioactive natural products from *Lysobacter*. *Nat. Prod. Rep.* **29**, 1277–1287 (2012).
11. L. Lou *et al.*, Biosynthesis of HSAF, a tetramic acid-containing macrolactam from *Lysobacter enzymogenes*. *J. Am. Chem. Soc.* **133**, 643–645 (2011).
12. T. A. Klein, S. Ahmad, J. C. Whitney, Contact-dependent interbacterial antagonism mediated by protein secretion machines. *Trends Microbiol.* **28**, 387–400 (2020).
13. J. H. Chang, D. Desveaux, A. L. Creason, The ABCs and 123s of bacterial secretion systems in plant pathogenesis. *Annu. Rev. Phytopathol.* **52**, 317–345 (2014).
14. X. Shen *et al.*, *Lysobacter enzymogenes* antagonizes soilborne bacteria using the type IV secretion system. *Environ. Microbiol.* **23**, 4673–4688 (2021).
15. Q. Wu *et al.*, Unlocking the bacterial contact-dependent antibacterial activity to engineer a biocontrol alliance of two species from natural incompatibility to artificial compatibility. *Stress Biol.* **1**, 19 (2021).
16. J. Luo *et al.*, *Acinetobacter baumannii* kills fungi via a type VI DNase effector. *mBio* **14**, e0342022 (2023).
17. K. Trunk *et al.*, Coulthurst, The type VI secretion system deploys antifungal effectors against microbial competitors. *Nat. Microbiol.* **3**, 920–931 (2018).
18. P. Wang, H. Chen, G. Qian, F. Liu, LetR is a TetR family transcription factor from *Lysobacter* controlling antifungal antibiotic biosynthesis. *Appl. Microbiol. Biot.* **101**, 3273–3282 (2017).
19. H. Wang, Z. Wang, Z. Liu, K. Wang, W. Xu, Membrane disruption of *Fusarium oxysporum* f. sp. *niveum* induced by myriocin from *Bacillus amyloliquefaciens* LZN01. *Microb. Biotechnol.* **14**, 517–534 (2021).
20. Y. Zhao *et al.*, Control of wheat Fusarium head blight by heat-stable antifungal factor (HSAF) from *Lysobacter enzymogenes*. *Plant Dis.* **103**, 1286–1292 (2019).
21. S. Li, L. Du, G. Yuen, S. D. Harris, Distinct ceramide synthases regulate polarized growth in the filamentous fungus *Aspergillus nidulans*. *Mol. Biol. Cell* **17**, 1218–1227 (2006).
22. S. Li, A. M. Calvo, G. Y. Yuen, L. Du, S. D. Harris, Induction of cell wall thickening by the antifungal compound dihydromaltophilin disrupts fungal growth and is mediated by sphingolipid biosynthesis. *J. Eukaryot. Microbiol.* **56**, 182–187 (2009).
23. W. R. Rittenour, M. Chen, E. B. Cahoon, S. D. Harris, Control of glucosylceramide production and morphogenesis by the Bar1 ceramide synthase in *Fusarium graminearum*. *PloS ONE* **6**, e19385 (2011).
24. F. He *et al.*, Transcriptomics analysis of the Chinese pear pathotype of *Alternaria alternata* gives insights into novel mechanisms of HSAF antifungal activities. *Int. J. Mol. Sci.* **19**, 1841 (2018).
25. Z. Liu *et al.*, A phosphorylated transcription factor regulates sterol biosynthesis in *Fusarium graminearum*. *Nat. Commun.* **10**, 1228 (2019).
26. C. Wang *et al.*, Functional analysis of the kinome of the wheat scab fungus *Fusarium graminearum*. *PLoS Pathog.* **7**, e1002460 (2011).
27. Y. Zhang *et al.*, Cellular tracking and gene profiling of *Fusarium graminearum* during maize stalk rot disease development elucidates its strategies in confronting phosphorus limitation in the host apoplast. *PLoS Pathog.* **12**, e1005485 (2016).
28. M. Yang *et al.*, An intrinsic mechanism for coordinated production of the contact-dependent and contact-independent weapon systems in a soil bacterium. *PLoS Pathog.* **16**, e1008967 (2020).
29. T. Gao *et al.*, The fungicidal activity of thymol against *Fusarium graminearum* via inducing lipid peroxidation and disrupting ergosterol biosynthesis. *Molecules* **21**, 770 (2016).
30. S. Ipcho *et al.*, Fungal innate immunity induced by bacterial microbe-associated molecular patterns (MAMPs). *G3 (Bethesda)* **6**, 1585–1595 (2016).
31. A. Quarantin *et al.*, Different hydrophobins of *Fusarium graminearum* are involved in hyphal growth, attachment, water-air interface penetration and plant infection. *Front. Microbiol.* **10**, 751 (2019).
32. A. Traven, B. Jelicic, M. Sopta, Yeast Gal4: A transcriptional paradigm revisited. *EMBO Rep.* **7**, 496–499 (2006).
33. M. M. Shneider *et al.*, PAAR-repeat proteins sharpen and diversify the type VI secretion system spike. *Nature* **500**, 350–353 (2013).
34. J. Wang *et al.*, The conserved domain database in 2023. *Nucleic Acids Res.* **51**, 384–388 (2023).
35. M. Varadi *et al.*, AlphaFold protein structure database: Massively expanding the structural coverage of protein-sequence space with high-accuracy models. *Nucleic Acids Res.* **50**, D439–D444 (2022).
36. D. Jurėnas *et al.*, Mounting, structure and autocleavage of a type VI secretion–associated Rhs polymorphic toxin. *Nat. Commun.* **12**, 6998 (2021).
37. X. Yan *et al.*, Transcriptional regulator PhlH modulates 2,4-diacetylphloroglucinol biosynthesis in response to the biosynthetic intermediate and end product. *Appl. Environ. Microbiol.* **83**, e01419–17 (2017).
38. B. Wang *et al.*, Targeted isolation of biocontrol agents from plants through phytopathogen co-culture and pathogen enrichment. *Phytopathol. Res.* **4**, 19 (2022).
39. N. Nachmias *et al.*, Systematic discovery of antibacterial and antifungal bacterial toxins. *Nat. Microbiol.* **9**, 3041–3058 (2024), https://doi.org/10.1101/2021.10.19.465003.
40. A. Deveau *et al.*, Bacterial–fungal interactions: Ecology, mechanisms and challenges. *FEMS Microbiol. Rev.* **42**, 335–352 (2018).
41. B. N. Steffan, N. Venkatesh, N. P. Keller, Let's get physical: Bacterial-fungal interactions and their consequences in agriculture and health. *J. Fungi (Basel)* **6**, 243 (2020).
42. Y. Zhang, E. K. Kastman, J. S. Guasto, B. E. Wolfe, Fungal networks shape dynamics of bacterial dispersal and community assembly in cheese rind microbiomes. *Nat. Commun.* **9**, 336 (2018).
43. L. P. Partida-Martinez, C. Hertweck, Pathogenic fungus harbours endosymbiotic bacteria for toxin production. *Nature* **437**, 884–888 (2005).
44. B. T. Ho, T. G. Dong, J. J. Mekalanos, A view to a kill: The bacterial type VI secretion system. *Cell Host Microbe* **15**, 9–21 (2014).

45. N. H. Le, V. Pinedo, J. Lopez, F. Cava, M. F. Feldman, Killing of Gram-negative and Gram-positive bacteria by a bifunctional cell wall-targeting T6SS effector. *Proc. Nat. Acad. Sci. U.S.A.* **118**, e2106555118 (2021).
46. J. Monjaras Feria, M. A. Valvano, An overview of anti-eukaryotic T6SS effectors. *Front. Cell. Infect. Microbiol.* **10**, 584751 (2020).
47. J. Vacheron *et al.*, T6SS contributes to gut microbiome invasion and killing of an herbivorous pest insect by plant-beneficial *Pseudomonas protegens*. *ISME J.* **13**, 1318–1329 (2019).
48. K. Xu, L. Lin, D. Shen, S. H. Chou, G. Qian, Clp is a "busy" transcription factor in the bacterial warrior, *Lysobacter enzymogenes*. *Comput. Struct. Biotechnol. J.* **19**, 3564–3572 (2021).
49. L. Lin *et al.*, Antifungal weapons of *Lysobacter*, a mighty biocontrol agent. *Environ. Microbiol.* **23**, 5704–5715 (2021).
50. G. L. Qian *et al.*, *Lysobacter enzymogenes* uses two distinct cell-cell signaling systems for differential regulation of secondary-metabolite biosynthesis and colony morphology. *Appl. Environ. Microbiol.* **79**, 6604–6616 (2013).
51. A. M. Fulano *et al.*, Functional divergence of flagellar type III secretion system: A case study in a non-flagellated, predatory bacterium. *Comput. Struct. Biotechnol. J.* **1**, 3368–3376 (2020).
52. L. Lin *et al.*, Data from "RNA-Seq of *Fusarium graminearum* PH-1 conidia treated with *Lysobacter enzymogenes* OH11". NCBI. https://www.ncbi.nlm.nih.gov/bioproject/PRJNA971132. Deposited 10 May 2023.
53. L. Lin *et al.*, Data from "*Microbiome* changes of banana soil treated with *Lysobacter enzymogenes*." NCBI. https://www.ncbi.nlm.nih.gov/bioproject/PRJNA1158950. Deposited 10 Sep 2024.
54. L. Lin *et al.*, Data from "Pseudomonas fulva strain:FoE9 Genome sequencing." NCBI. https://www.ncbi.nlm.nih.gov/bioproject/PRJNA1158498. Deposited 8 Sep 2024.